International Journal of Heat and Mass Transfer 84 (2015) 671–679

Contents lists available at ScienceDirect

International Journal of Heat and Mass Transfer

journal homepage: www.elsevier.com/locate/ijhmt

A time step amplification method in boundary face method for transient heat conduction

Fenglin Zhou [a,b], Yuan Li [a], Jianming Zhang [a,*], Cheng Huang [a], Chenjun Lu [a]

[a] State Key Laboratory of Advanced Design and Manufacturing for Vehicle Body, College of Mechanical and Vehicle Engineering, Hunan University, Changsha 410082, China
[b] Modern Jetting Department, Hunan University of Technology, Zhuzhou 412001, China

ARTICLE INFO

Article history:
Received 27 May 2013
Received in revised form 1 January 2015
Accepted 11 January 2015

Keywords:
Small time step
Numerical instability
Time domain boundary integral equation
Transient heat conduction

ABSTRACT

A time domain boundary integral equation method, which is named as quasi-initial condition method, is applied in this paper to solve the transient heat conduction problem. In conventional implementations, however, this method suffers from a numerically unstable problem when the time step is small. To improve the numerical stability of the method, a time step amplification method is proposed. In the proposed method, an amplified time step is adopted to compute the temperature and the flux at the virtual time point. The boundary condition at that virtual time point is determined through a linear interpolation by the conditions at the current time step point and the quasi-initial time. Furthermore, the heat generation in the virtual time step is assumed to be constant which is the same as that in the real time step. The temperature and the flux at the current step time point are then computed through a linear interpolation over the time interval. A short but not rigorous deduction of this method is presented to show that this method is valid in solution to problems in which the temperature and the flux vary linearly respect to time. Numerical examples further demonstrate the numerical stability of the proposed method.

1. Introduction

The transient heat conduction problem widely appears in engineering problems. Many numerical methods have been proposed to solve this problem such as the finite difference method (FDM) [1,2], the finite volume method (FVM) [3,4], the finite element method (FEM) [5,6] and the boundary element method (BEM) [7–17]. Among these methods, the BEM seems to be more attractive for its dimension reduction feature. For transient heat conduction problem, BEM may be classified into two catalogs: the transformed domain method [7–9] and the time domain method [10–17]. The transformed method usually leads to an accurate result. In that method, however, it is very difficult to determine the transformation parameters which play a great important role in the numerical scheme. Moreover, for many practical problems, a large number of sampling frequencies is often required to obtain accurate solutions. Hence the numerical inverse transformation is usually very time-consuming and the accelerated techniques should be employed [7,8].

In this paper, we concern the time domain method. There are two different implementations of time domain methods. One employs the time-independent fundamental solution and the other one employs the time-domain fundamental solution. In the case of time-independent fundamental solution, the derivatives with respect to temporal variable are treated through a time domain difference scheme. In that implementation, domain integrals of the temperature are involved and the computational scale is related to the number of domain nodes. Thus, it lost the advantages of dimension reduction in the BIE method.

The numerical method employing the time-domain fundamental solution was first used by Thaler et al. in [10]. In Brebbia's work [11], this type of method is further classified into two schemes. One is named by convolution quadrature method (CQM) and the other one is the quasi-initial condition method. In the CQM, temperature and flux at each step are computed through a convolution of temperature and flux on the boundary at previous steps. If the initial temperature and the heat generation are omitted, the CQM leads to a pure boundary method. As indicated in [12–16], however, the CQM suffers from the time-consuming convolution especially in the case that a long time history is concerned. Many methods were proposed to accelerate the computation of the convolution. Gupta et al. applied an expanded fundamental solution to reduce the calculation of boundary integrals that appear in the time convolution [13]. Considering the decay of the time domain fundamental solution, Banerjee et al. developed an efficient time

* Corresponding author. Tel.: +86 731 88823061.
E-mail address: zhangjm@hnu.edu.cn (J. Zhang).

http://dx.doi.org/10.1016/j.ijheatmasstransfer.2015.01.060
0017-9310/

domain convolution method in which the number of integral points was determined adaptively [14]. By combining with the boundary face method [18–22], Zhou et al. applied the efficient time domain convolution method to analyze structures with open-ended tubular holes [15]. If the initial temperature or the heat generation is not negligible, however, two methods lost their dimension reduction advances.

In this paper, we will implement the quasi-initial condition method to solve transient heat conduction problem. In this method, the temperature which is computed in the previous step is treated as the initial temperature in current step. Thus, the domain integral of this initial temperature is involved in the BIE. Compared with the CQM, however, time consuming convolution is avoided in this method. Furthermore, in our implementation, the scale of corresponding systems which should be solved is just related to the number of boundary nodes and is independent of the number of domain nodes.

As pointed out in [23–25], the quasi-initial condition method becomes numerically unstable for small time step. Iso and Onishi discussed the unstable problem in [23]. Sharp studied the unstable problem in 1D case through matrix analysis [24]. Peirce et al. studied this problem through a Fourier transformation tool [25]. In the above works, authors tried to find the pre-condition to judge if the computation was stable. In many engineering applications, small time step should be considered.

In this paper, a time step amplification method is developed to improve the numerical stability. In this method, the time step is first amplified into a larger time step. Temperatures and fluxes at the virtual time step point are then computed. Temperatures and fluxes at the actual time step point are finally computed by applying a linear interpolation scheme in the time interval. In the computation of temperatures and fluxes at the virtual time step point, the corresponding boundary condition is interpolated by the boundary condition of actual time step point and that of the initial time point. We will prove theoretically that the temperatures and fluxes obtained by the proposed method satisfy both the governing equation and the boundary condition. Since the time step which is involved in the systems is the amplified one, the proposed method can improve the numerical stability of the solution.

Three numerical examples are presented to verify the stability of the proposed method. It is worth noting that in the last example, a practical engineering problem is considered. Comparison with the available finite element software is made, showing the ability of the proposed method in practical application.

2. The time domain boundary integral equation for transient heat conduction

This section introduces the time domain boundary integral equation for the transient heat conduction. We start from the governing equation of heat conduction problem in isotropic media:

$$\begin{aligned} &k\nabla^2 u(x,t) + Q(x,t) = \rho c \frac{\partial}{\partial t} u(x,t), \quad \forall x \in \Omega \\ &u(x,t) = \bar{u}(x,t), \quad \forall x \in \Gamma_d \\ &-k\frac{\partial u(x,t)}{\partial n} \equiv q(x,t) = \bar{q}(x,t), \quad \forall x \in \Gamma_n \\ &u(x,t_0) = u_0(x), \quad \forall x \in \Omega \end{aligned} \tag{1}$$

where the domain Ω is enclosed by $\Gamma = \Gamma_d \cup \Gamma_n$ as shown in Fig. 1, material properties k, ρ, c stand for conductivity, density and specific heat, respectively. u, q denote the temperature and heat flux. Q denotes the heat generation inside the domain. $\bar{u}$, $\bar{q}$ is prescribed temperature and heat flux on the boundary. n stands for the outward normal on the boundary. t_0 is the initial time. It should be noted that the material which we concern in this paper is homogeneous.

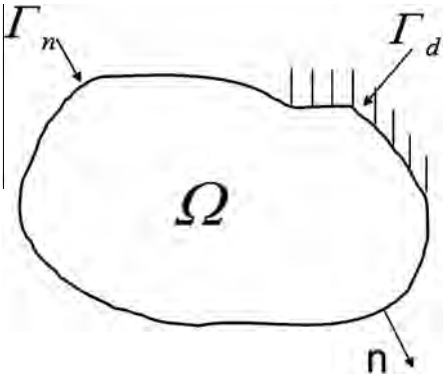

Fig. 1. Boundary conditions of heat conduction problem.

The problem can be converted into an equivalent BIE which is described as the following formulation [11]:

$$\begin{aligned} C(y)u(y,\tau) = &\frac{1}{\rho c}\int_0^\tau \int_\Gamma u(x,t)q^*(y,x;\tau,t)d\Gamma(x)dt \\ &-\frac{1}{\rho c}\int_0^\tau \int_\Gamma u^*(y,x;\tau,t)q(x,t)d\Gamma(x)dt \\ &+\int_\Omega u^*(y,x;\tau,0)u(x,0)d\Omega(x) \\ &+\frac{1}{\rho c}\int_0^\tau \int_\Omega u^*(y,x;\tau,t)Q(x,t)d\Omega(x)dt \end{aligned} \tag{2}$$

In this formula, y and x respectively stand for the field point and source point. And

$$C(y) = \begin{cases} 0 & y \in \bar{\Omega} \\ 1 & y \in \Omega \\ \frac{\theta}{2\pi} & y \in \Gamma \end{cases} \tag{3}$$

in which θ is the solid angle of the boundary at collocation point y and $\theta = \pi$ when the boundary near y is smooth. $u^*(y,x;\tau,t)$ and $q^*(y,x;\tau,t)$are the fundamental solutions which can be respectively written as

$$u^*(y,x;\tau,t) = \frac{H(\tau-t)}{(4\pi K(\tau-t))^{1.5}} e^{\frac{-r^2}{4K(\tau-t)}} \tag{4}$$

and

$$q^*(y,x;\tau,t) = -k\frac{\partial u^*(y,x;\tau,t)}{\partial n(x)} \tag{5}$$

Since the variations of temperature and heat flux with respect to both spatial variables and temporal variables are usually unknown, discretization both on space and time is required. We use a boundary face method, which is detailed in [18–22], to discretize the boundary of the considered domain. To compute the temperature and the flux step by step, a piece-wise linear Lagrange interpolation scheme together with a time-stepping scheme, which is named by quasi-initial condition scheme, are adopted.

3. Quasi-initial condition scheme for boundary integral equation

In the quasi-initial condition scheme, the temperature computed in the front step is considered as the initial condition in the current step. In each step, we first computed the temperature and flux on the boundary, and then we calculate the temperature on internal nodes. The time interval from 0 to τ can be divided into M increments of duration Δt. With the quasi-initial condition scheme, Eq. (2) has a time discretized form in the mth step:

$$C(y)u(y,t_m)=\frac{1}{\rho c}\int_{t_{m-1}}^{t_m}\int_{\Gamma}u(x,t)q^*(y,x;t_m,t)d\Gamma(x)dt-\frac{1}{\rho c}\int_{t_{m-1}}^{t_m}\int_{\Gamma}u^*(y,x;\tau,t)q(x,t)d\Gamma(x)dt+\int_{\Omega}u^*(y,x;t_m,t_{m-1})u(x,t_{m-1})d\Omega(x)+\frac{1}{\rho c}\int_{t_{m-1}}^{t_m}\int_{\Omega}u^*(y,x;t_m,t)Q(x,t)d\Omega(x)dt \tag{6}$$

in which $t_m=t_{m-1}+\Delta t$. In this application, the variation of temperature and flux with respect to time are approximated by a linear function

$$u(x,t)=\frac{t_m-t}{\Delta t}u^{m-1}(x)+\frac{t-t_{m-1}}{\Delta t}u^m(x)\quad t\in(t_{m-1},t_m) \tag{7}$$

$$q(x,t)=\frac{t_m-t}{\Delta t}q^{m-1}(x)+\frac{t-t_{m-1}}{\Delta t}q^m(x)\quad t\in(t_{m-1},t_m) \tag{8}$$

And the heat generation is assumed to be steady in this time interval.

$$Q(x,t)=\bar{Q}^m(x)=\int_{t_{m-1}}^{t_m}Q(x,t)dt\quad t\in(t_{m-1},t_m) \tag{9}$$

With this linear interpolation, Eq. (6) is converted into

$$C(y)u(y,t_m)=\frac{1}{\rho c}\int_{\Gamma}(u^m(x)\int_{t_{m-1}}^{t_m}q^*(y,x;t_m,t)\frac{t-t_{m-1}}{\Delta t}dt+u^{m-1}(x)\int_{t_{m-1}}^{t_m}q^*(y,x;t_m,t)\frac{t_m-t}{\Delta t}dt)d\Gamma(x)-\frac{1}{\rho c}\int_{\Gamma}(q^m(x)\int_{t_{m-1}}^{t_m}u^*(y,x;\tau,t)\frac{t-t_{m-1}}{\Delta t}dt+q^{m-1}(x)\int_{t_{m-1}}^{t_m}u^*(y,x;\tau,t)\frac{t_m-t}{\Delta t}dt)d\Gamma(x)+\frac{1}{\rho c}\int_{\Omega}\bar{Q}^m(x)\int_{t_{m-1}}^{t_m}u^*(y,x;t_m,t)dtd\Omega(x)+\int_{\Omega}u^*(y,x;t_m,t_{m-1})u(x,t_{m-1})d\Omega(x) \tag{10}$$

For boundary discretization, we assume on the boundary that

$$u^m(u,v)=\sum_{k=1}^{N}N_k(u,v)u_k^m \tag{11}$$

and

$$q^m(u,v)=\sum_{k=1}^{N}N_k(u,v)q_k^m \tag{12}$$

In order to calculate the domain integrals of initial temperature, which appear in the right hand side of Eq. (10), the initial temperature inside the domain are approximated through:

$$u^{m-1}(x)=\sum_{l=1}^{L}\Phi_l(x)u_l^{m-1} \tag{13}$$

where $\Phi_l(x)$ is the lth shape function and L is the number of interpolation points inside the domain.

In this application, we assume that the heat generation varies only respect to temporal variable but not respect to spatial variable. In another word, we should keep in mind

$$Q(x,t)=Q(t)=\overline{Q}^m=\int_{t_{m-1}}^{t_m}Q(t)dt\quad t\in(t_{m-1},t_m) \tag{14}$$

Since the heat generation is constant all over the domain, the domain integral of the heat generation in Eq. (10) can be converted to a boundary integral through the divergence theorem.

$$\int_{\Omega}\overline{Q}^m(x)\int_{t_{m-1}}^{t_m}u^*(y,x;t_m,t)dtd\Omega(x)=\overline{Q}^m\int_{\Gamma}A^*(y,x;t_m)d\Gamma(x) \tag{15}$$

in which

$$\frac{\partial}{\partial n(x)}A^*(y,x;t_m)=\int_{t_{m-1}}^{t_m}u^*(y,x;t_m,t)dt \tag{16}$$

Substitute Eqs. (11)–(13) and (15) into Eq. (10), we will obtain

$$C(y)u(y,t_m)=\frac{1}{\rho c}\sum_{j=1}^{BE}\sum_{k=1}^{N}u_k^m\int_{\Gamma_j}N_k(x)\int_{t_{m-1}}^{t_m}q^*(y,x;t_m,t)\times\frac{t-t_{m-1}}{\Delta t}dtd\Gamma(x)+\frac{1}{\rho c}\sum_{j=1}^{BE}\sum_{k=1}^{N}u_k^{m-1}\int_{\Gamma_j}N_k(x)\times\int_{t_{m-1}}^{t_m}q^*(y,x;t_m,t)\frac{t_m-t}{\Delta t}dtd\Gamma(x)-\frac{1}{\rho c}\sum_{j=1}^{BE}\sum_{k=1}^{N}q_k^m\int_{\Gamma_j}N_k(x)\int_{t_{m-1}}^{t_m}u^*(y,x;t_m,t)\times\frac{t-t_{m-1}}{\Delta t}dtd\Gamma(x)-\frac{1}{\rho c}\sum_{j=1}^{BE}\sum_{k=1}^{N}q_k^{m-1}\int_{\Gamma_j}N_k(x)\times\int_{t_{m-1}}^{t_m}u^*(y,x;t_m,t)\frac{t_m-t}{\Delta t}dtd\Gamma(x)+\frac{1}{\rho c}\sum_{j=1}^{BE}\sum_{k=1}^{N}\bar{Q}_k^m\int_{\Gamma_j}N_k(x)A^*(y,x;t_m)d\Omega(x)+\sum_{jj=1}^{DE}\sum_{l=1}^{L}u_l^{m-1}\int_{\Omega_{jj}}\Phi_l(x)u^*(y,x;t_m,t_{m-1})d\Omega(x) \tag{17}$$

in which BE, DE denote the number of boundary elements and the number of domain elements. Furthermore, we denote

$$U_m^*(y,x)=\int_{t_{m-1}}^{t_m}u^*(y,x;t_m,t)\frac{t-t_{m-1}}{\Delta t}dt \tag{18}$$

$$U_{m-1}^*(y,x)=\int_{t_{m-1}}^{t_m}u^*(y,x;t_m,t)\frac{t_m-t}{\Delta t}dt \tag{19}$$

$$P_m^*(y,x)=\int_{t_{m-1}}^{t_m}q^*(y,x;t_m,t)\frac{t-t_{m-1}}{\Delta t}dt \tag{20}$$

$$P_{m-1}^*(y,x)=\int_{t_{m-1}}^{t_m}q^*(y,x;t_m,t)\frac{t_m-t}{\Delta t}dt \tag{21}$$

Eq. (17) becomes

$$C(y)u(y,t_m)=\frac{1}{\rho c}\sum_{j=1}^{BE}\sum_{k=1}^{N}u_k^m\int_{\Gamma_j}N_k(x)P_m^*(y,x)d\Gamma(x)+\frac{1}{\rho c}\sum_{j=1}^{BE}\sum_{k=1}^{N}u_k^{m-1}\int_{\Gamma_j}N_k(x)P_{m-1}^*(y,x)d\Gamma(x)-\frac{1}{\rho c}\sum_{j=1}^{BE}\sum_{k=1}^{N}q_k^m\int_{\Gamma_j}N_k(x)U_m^*(y,x)d\Gamma(x)-\frac{1}{\rho c}\sum_{j=1}^{BE}\sum_{k=1}^{N}q_k^{m-1}\int_{\Gamma_j}N_k(x)U_{m-1}^*(y,x)d\Gamma(x)+\frac{1}{\rho c}\sum_{j=1}^{BE}\sum_{k=1}^{N}\bar{Q}_k^m\int_{\Gamma_j}N_k(x)A^*(y,x;t_m)d\Omega(x)+\sum_{jj=1}^{DE}\sum_{l=1}^{L}u_l^{m-1}\int_{\Omega_{jj}}\Phi_l(x)u^*(y,x;t_m,t_{m-1})d\Omega(x) \tag{22}$$

Then we collocate y at each boundary node, we have the following system

$$\mathbf{G}_m^{bb}\mathbf{q}_m^b - \mathbf{H}_m^{bb}\mathbf{u}_m^b = \mathbf{H}_{m-1}^{bb}\mathbf{u}_{m-1}^b - \mathbf{G}_{m-1}^{bb}\mathbf{q}_{m-1}^b + \mathbf{S}_m^{bb}\mathbf{Q}_m^b + \mathbf{D}_m^{bd}\mathbf{u}_{m-1}^d \quad (23)$$

in which, the superscript b, d denote the boundary node and the domain node, and

$$H_{ik}^m = \frac{1}{\rho c}\sum_{j=1}^{BE}\int_{\Gamma_j} P_m^*(y_i,x)N_k(x)d\Gamma(x) \quad (24)$$

$$G_{ik}^m = \frac{1}{\rho c}\sum_{j=1}^{BE}\int_{\Gamma_j} U_m^*(y_i,x)N_k(x)d\Gamma(x) \quad (25)$$

$$D_{il}^m = \sum_{jj=1}^{DE}\int_{\Omega_{jj}} u^*(y_i,x;t_m,t_{m-1})\Phi_l(x)d\Omega(x) \quad (26)$$

$$S_{ik}^m = \frac{1}{\rho c}\sum_{j=1}^{BE}\sum_{k=1}^{N}\int_{\Gamma_j} N_k(x)A^*(y_i,x;t_m)d\Omega(x) \quad (27)$$

With considering the boundary condition, Eq. (23) can be solved to compute the unknown temperature or flux on the boundary nodes. Then we should calculate temperature inside the domain, which will be considered as initial temperature of the next time step. To calculate the temperature at domain nodes, we collocate y on each domain nodes and the following formula should be applied.

$$\mathbf{u}_m^d = \mathbf{H}_m^{db}\mathbf{u}_m^b - \mathbf{G}_m^{db}\mathbf{q}_m^b + \mathbf{H}_{m-1}^{db}\mathbf{u}_{m-1}^b - \mathbf{G}_{m-1}^{db}\mathbf{q}_{m-1}^b + \mathbf{S}_m^{db}\mathbf{Q}_m^b + \mathbf{D}_m^{dd}\mathbf{u}_{m-1}^d \quad (28)$$

It is worth noting that the matrix in Eqs. (23) and (28) stays the same if the length of time step remains the same. Eq. (23) should only be solved once in the first time step. Eq. (28) contains only the matrix–vector multiplication. In other steps, the inversed matrix, which is computed in the first step, is stored. Thus the solution for Eq. (23) in other steps can also be achieved by a series of matrix–vector multiplication.

The quasi-initial condition scheme is obviously more efficient than the time stepping convolution scheme especially for long time history case. As indicated in many literatures, this scheme is numerically unstable when the increment is small [24,25]. In this paper, a time step amplification method, which will be described in the following section, is proposed to solve this problem.

4. The time step amplification method

We have investigated the influence of Δt on the stability of results by case studies. It was found that only a small range of Δt resulted in acceptable results, which can be determined by the following formula

$$L^2/4K \leqslant \Delta t \leqslant L^2/K \quad (29)$$

in which L represents the characteristic space-element length, $K = k/c\rho$ is the diffusion coefficient and Δt is the time step length.

In heat conduction problems, the variations of the temperature and the flux inside the domain with respect to time are caused by two main factors. One is the variation of boundary condition. The other one is the heat generation. In the time step amplification method, the origin time step is amplified into a virtual step with a larger increment. The boundary condition at the virtual step time point is computed through a linear amplification of that at the origin step time point. The heat generation in the virtual time step is the same as that in the origin time step. The boundary temperature, flux and domain temperature at the virtual step time point is firstly computed. Then the corresponding quantities at the origin virtual time step time points are computed through a simple linear interpolation within the virtual time step interval.

Fig. 2 shows intervals of the origin time step $[t_0,\tau]$ and the virtual time step $[t_0,t_1]$.

In the case that the temperature inside the domain varies linearly with respect to time, and that the heat generation is constant all over the domain, the solution to a heat conduction problem with Dirichlet boundary satisfies

$$\frac{\partial}{\partial t}u(x,t) = g(x) \quad (30)$$

At the time t_0, t_1, Eq. (30) satisfies the governing equation of the heat conduction problem (at the time point, the problem can be considered as a boundary value problem).

$$K\nabla^2 u(x,t_0) + \frac{Q}{\rho c} = g(x) \quad (31)$$

$$K\nabla^2 u(x,t_1) + \frac{Q}{\rho c} = g(x) \quad (32)$$

And the boundary condition at time t_0 and t_1 are

$$u(x,t_0) = \bar{u}_0(x) \quad \forall x \in \Gamma \quad (33)$$

$$u(x,t_1) = \bar{u}_1(x) \quad \forall x \in \Gamma \quad (34)$$

In the time step amplification method, the boundary condition at t_1 satisfies

$$\bar{u}_1(x) = \frac{\tau - t_1}{\tau - t_0}\bar{u}_0(x) + \frac{t_1 - t_0}{\tau - t_0}\bar{u}_\tau(x) \quad \forall x \in \Gamma \quad (35)$$

the solution at time τ is computed through a linear interpolation which is

$$u(x,\tau) = \frac{t_1 - \tau}{t_1 - t_0}u(x,t_0) + \frac{\tau - t_0}{t_1 - t_0}u(x,t_1) \quad (36)$$

On the boundary we have the following relation

$$\begin{aligned} u(x,\tau) &= \frac{t_1 - \tau}{t_1 - t_0}u(x,t_0) + \frac{\tau - t_0}{t_1 - t_0}u(x,t_1) \\ &= \frac{t_1 - \tau}{t_1 - t_0}\bar{u}_0(x) + \frac{\tau - t_0}{t_1 - t_0}\bar{u}_1(x) \\ &= \frac{t_1 - \tau}{t_1 - t_0}\bar{u}_0(x) + \frac{\tau - t_0}{t_1 - t_0}\left[\frac{\tau - t_1}{\tau - t_0}\bar{u}_0(x) + \frac{t_1 - t_0}{\tau - t_0}\bar{u}_\tau(x)\right] \\ &= \bar{u}_\tau(x) \quad \forall x \in \Gamma \end{aligned} \quad (37)$$

For inner domain points, we have the following relation

$$\begin{aligned} K\nabla^2 u(x,\tau) + \frac{Q}{\rho c} &= K\nabla^2\left(\frac{t_1 - \tau}{t_1 - t_0}u(x,t_0) + \frac{\tau - t_0}{t_1 - t_0}u(x,t_1)\right) + \frac{Q}{\rho c} \\ &= \frac{t_1 - \tau}{t_1 - t_0}K\nabla^2 u(x,t_0) + \frac{\tau - t_0}{t_1 - t_0}K\nabla^2 u(x,t_1) + \frac{Q}{\rho c} \\ &= \frac{t_1 - \tau}{t_1 - t_0}\left[K\nabla^2 u(x,t_0) + \frac{Q}{\rho c}\right] \\ &\quad + \frac{\tau - t_0}{t_1 - t_0}\left[K\nabla^2 u(x,t_1) + \frac{Q}{\rho c}\right] = \frac{t_1 - \tau}{t_1 - t_0}g(x) \\ &\quad + \frac{\tau - t_0}{t_1 - t_0}g(x) = g(x) \end{aligned} \quad (38)$$

As illustrated in Eqs. (37) and (38), the solution obtained by the time step amplification method satisfies both the boundary condition and the governing differential equation. Thus we believe that the temperature obtained by the time step amplification method is the solution to the considered heat conduction problem.

Fig. 2. Time interval of origin and amplified time step.

5. Numerical examples

In this section, three numerical examples will be presented to verify the stability of the proposed method. In these examples, the relative errors are defined as:

$$E_r = \sqrt{\frac{1}{N}\sum_{i=1}^{N}\left(v_i^{(e)} - v_i^{(n)}\right)^2} \tag{39}$$

in which the superscripts (e) and (n) refer to the exact and numerical solutions respectively.

5.1. Suddenly heated cube

In this example, we concern a unit cube which is suddenly heated on one surface. Other surfaces are insulated. The thermal conductivity, the heat capacity and the density of the cube are 0.5 W/(m °C), 0.5 J/(kg °C) and 8.0 kg/m^3, respectively. The length of the cube is 1 m. The corresponding boundary conditions are illustrated in Fig. 3.

A uniform temperature boundary (100 °C) is imposed suddenly on the top face of the cube. The initial temperature of the cube is 0 °C. In this application, the variation history of the temperature from 0 s to 9.6 s at the bottom surface is concerned. Four kinds of time step including 0.1 s, 0.2 s, 0.4 s and 0.8 s are employed. In this implementation, we have also applied the time step amplification method to circumvent the unstable problem. To illustrate the accuracy of the method, numerical results are compared with the existing analytical solution to the considered problem. Fig. 4 shows the results that are obtained by using time step 0.1 s.

In Fig. 4, the line with 0.1×1 denotes for the result which is obtained by the direct quasi-initial condition method without the time step amplification. The lines with 0.1×2, 0.1×4 and 0.1×8 represent the result which is obtained by quasi-initial condition method with 2, 4 and 8 times amplified time step, respectively. It can be seen significantly that the numerical results break down. The quasi-initial condition method becomes unstable without the time step amplification when the time step length is 0.1 s. By using the time step amplification method, however, the accuracy of the result is significantly improved. And the quasi-initial condition method becomes more numerically stable. It is worth noting that in the first step, the accuracy has not been improved by the time step amplification method. This is because in this problem, the flux at the beginning of the time history is infinite. It is very hard to approximate this singular flux by conventional time approximation scheme. As suggested in [26], however, employing higher order time approximations may relieve this problem.

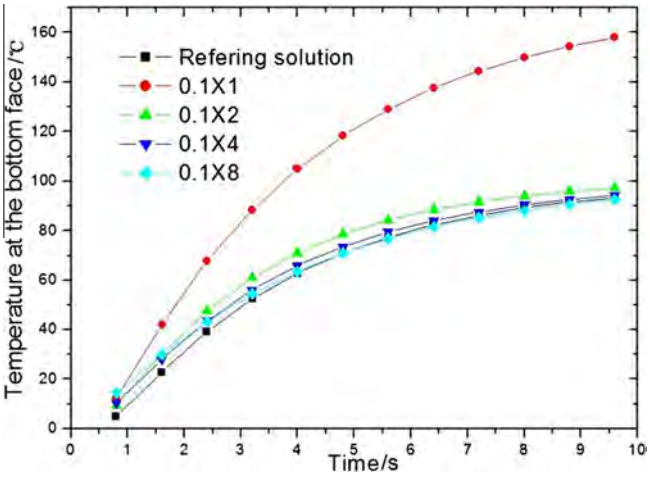

Fig. 4. Variation history of temperature on the bottom face obtained using 0.1 s time step.

To further demonstrate the accuracy of the time step amplification method, Fig. 5 illustrates the results that are obtained by using time step 0.4 s and 0.8 s.

From Fig. 5, it can be seen that the result which is obtained by direct quasi-initial condition method with time step 0.8×1 s is less accurate than that obtained by using time step 0.4×2 s. In other words, with the same time step length, the amplified time step leads to a better result.

5.2. heat conduction in a cylinder

In this example, we concern a cylinder with length 10 m and diameter 3 m. The location and geometry of the cylinder are illustrated in Fig. 6. The heat conductivity, specific heat and density of the cylinder are 1.0 W/(m °C), 1.0 J/(kg °C) and 1.0 kg/m^3, respectively. A uniform heat generation rate with a magnitude of 6 °C/s exists inside the cylinder.

A temperature boundary whose distribution can be described as the following function

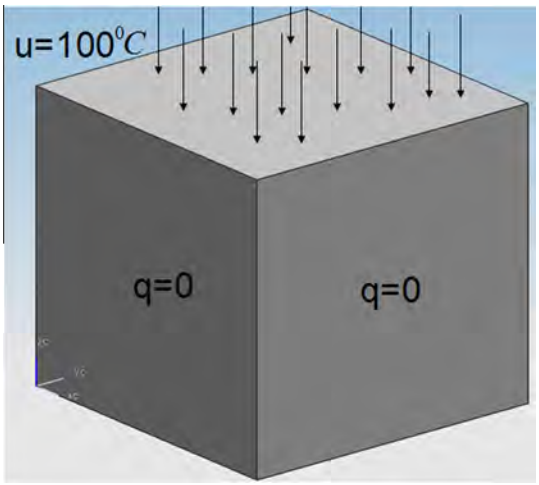

Fig. 3. A suddenly heated cube.

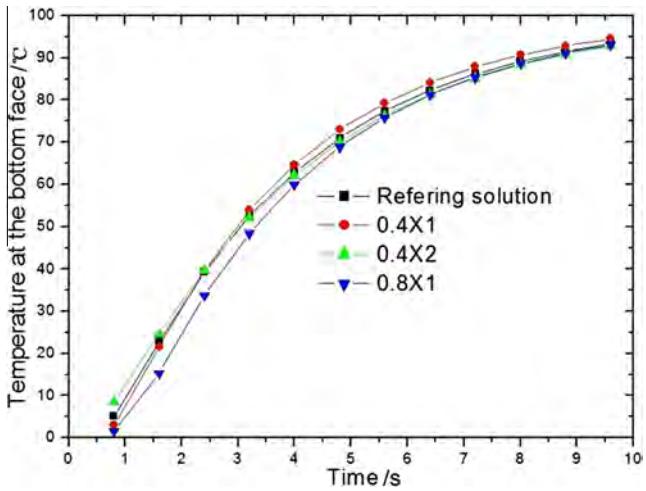

Fig. 5. Results obtained by using 0.4 s and 0.8 s time steps.

Fig. 6. Geometry of the cylinder.

$$u(x,y,z) = x^3 + 2y^3 + 1.5z^3 + (6x + 12y + 9z + 6)t\ (^\circ\mathrm{C}) \quad (x,y,z) \in \Gamma \tag{40}$$

is imposed on all the boundary surfaces. The initial temperature distribution is:

$$u(x,y,z) = x^3 + 2y^3 + 1.5z^3\ (^\circ\mathrm{C}) \quad (x,y,z) \in \Omega \tag{41}$$

We concern the temperature and flux variation history along 0s to 20s. The exact solution to this problem can be represented analytically by

$$u(x,y,z) = x^3 + 2y^3 + 1.5z^3 + (6x + 12y + 9z + 6)t\ (^\circ\mathrm{C}) \tag{42}$$

In this application, we subdivide the considered time interval 0–20 s into 400 increments. In each increment, the step length is 0.05 s. Flux results at boundary nodes are concerned and compared with the following exact flux distribution:

$$q(x,y,z) = -k\frac{\partial u(x,y,z)}{\partial \mathbf{n}} \quad (x,y,z) \in \Gamma \tag{43}$$

in which k stands for the heat conductivity of the material and $\boldsymbol{n}$ is the outward normal on the boundary node. The time step amplification scheme which we apply in this example is more adaptive. The amplified time step length is computed through the following expression:

$$\Delta t = \frac{\xi^2}{4Ka} \tag{44}$$

where ξ is the maximum size among all the elements including both boundary elements and domain elements. K is the thermal diffusivity of the material which is 1 m^2/s. a is a parameter which controls the length of the virtual time step. In this application, 590 quadratic boundary elements including both triangular and quadrilateral elements are employed and in total 1679 boundary nodes are involved as illustrated in Fig. 7. To calculate the domain integral of quasi-initial condition and the heat generation, this cylinder is discretized into 4122 linear tetra elements as illustrated in Fig. 8. And in total 990 domain nodes are involved.

A direct analysis without any time step amplification is firstly performed. Then a time step amplification scheme is applied to perform the analysis. In the time step amplification scheme, $a = 0.125$, $a = 0.0625$ and $a = 0.003125$ are applied, respectively. The maximum size of the elements is 0.5 m. The lengths of amplified time steps are actually 0.5 s, 1 s and 20 s which are 10, 20 and 400 times of the length of the considered time step, respectively.

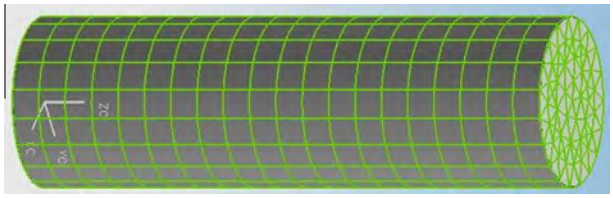

Fig. 7. Boundary elements on the cylinder.

Relative errors of normal flux on boundary nodes are illustrated in Fig. 9.

From Fig. 9, it can be seen that numerically unstable problem appears in the direct analysis with time step length 0.05 s. The relative error of boundary nodal q increases as time increases. By applying the time step amplification schemes, however, the numerical stability is significantly improved. Accurate result can be obtained even when the computational time step is amplified by 400 times. It should be noting that the normal flux at the initial time is computed through a numerical derivative of the initial

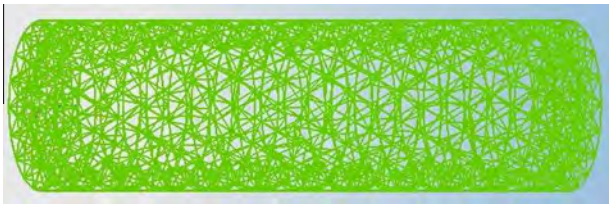

Fig. 8. Domain elements in the cylinder.

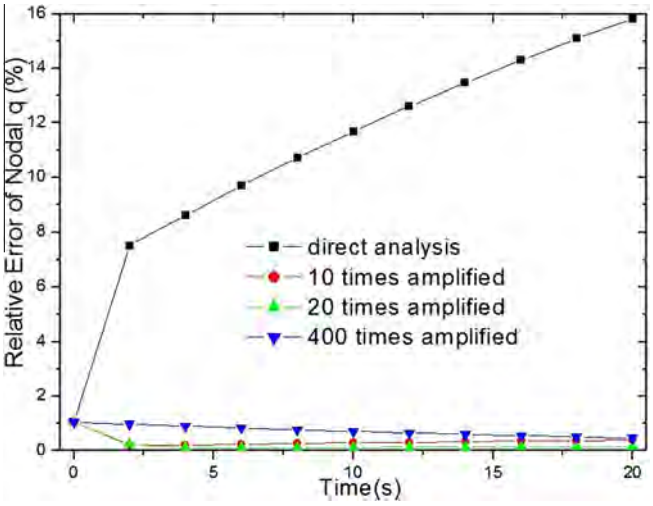

Fig. 9. Relative error of boundary nodal q.

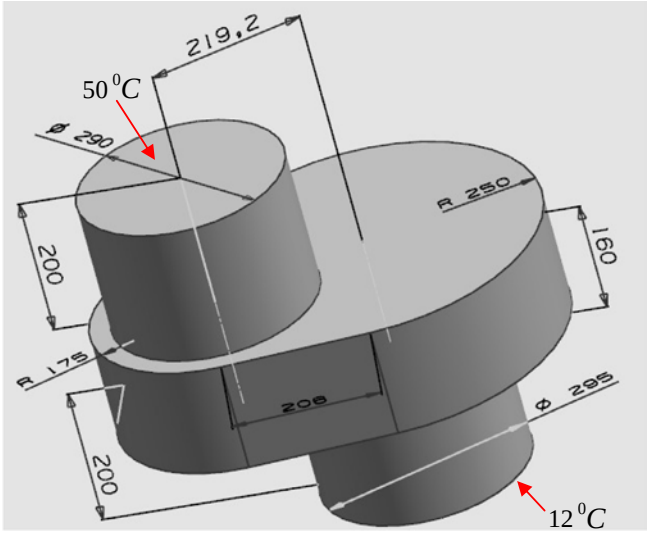

Fig. 10. The aluminum crankshaft.

temperature in all these implementations. Thus the relative errors of nodal q in these implementations coincide with each other. Since the exact temperature varies linearly with the time, a very large time step can also lead to an accurate result. In practical cases, however, the variation of the temperature according to time is much more complex. In those cases, a very large time step amplification scale is not suggested. This example further demonstrated the stability of the time step amplification method. To show the ability of the proposed method in engineering problem, a more practical problem will be considered in the following example.

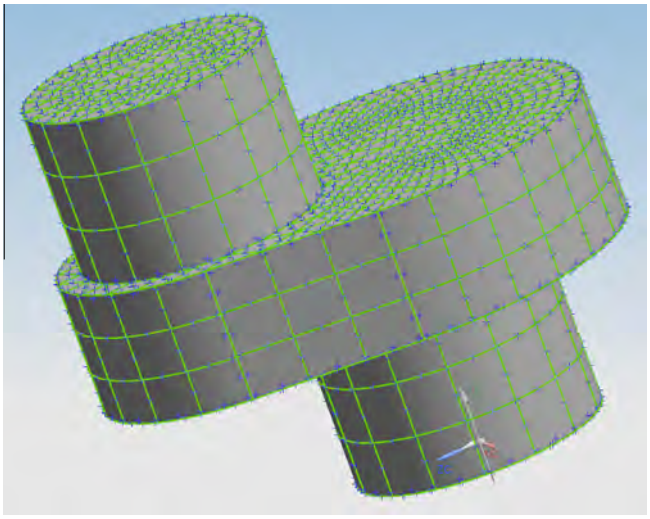

Fig. 11. Boundary elements and boundary nodes.

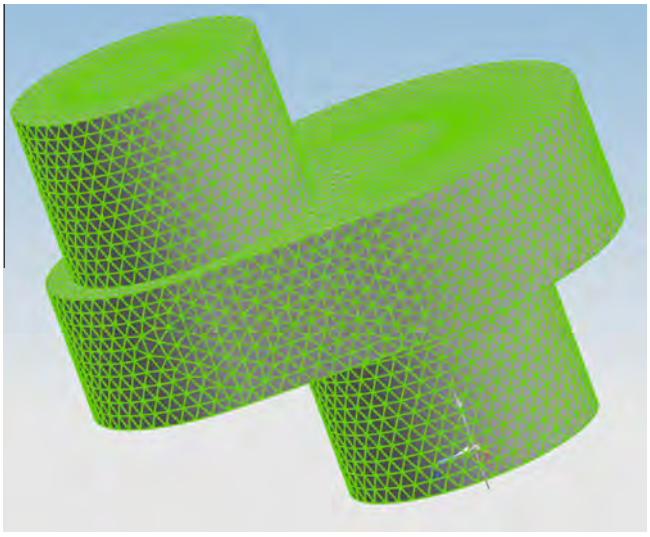

Fig. 12. Domain mesh for the crankshaft.

5.3. Heat conduction in an aluminum crankshaft

In the last example, an aluminum crankshaft as illustrated in Fig. 10 is concerned.

The density, the heat conductivity and the specific heat of the crankshaft are 0.00267 g/mm^3, 0.22795 J/(mm °C s) and 0.9211 J/(g °C), respectively. The crankshaft is occupied initially in the environment of 12 °C. Then suddenly a 50 °C is imposed on the top face of the crankshaft and the bottom face is kept 12 °C. Other faces are insulated. We concern the temperature variation history in the time interval [0 s, 1000 s]. In the BFM implementation for this problem, the time interval was divided into 100 time steps of which the increment is 10 s. The length of the amplified time step is computed through Eq. (44) in which the parameter $a = 1$ is assumed. 1137 quadratic elements which contain 3165 boundary nodes (Fig. 11) and 29,951 linear tetra elements (Fig. 12) involving in total 7212 domain nodes are employed in this application.

It is worth noting that both triangular elements and quadrangular elements are involved in the boundary elements. These mixed types of elements will not decrease the accuracy of the method. And this is a very attractive property of the BFM as indicated in [18,19]. In the BFM implementation, in total 121 s are consumed including 24 s for mesh generation and 97 s for computation.

On the other hand, a FEM implementation has also been performed to make comparisons with the BFM. The FEM implementation is performed through the commercial software ABAQUS with edition 11.1. In the FEM implementation, 51,954 quadratic tetra elements, which contain in total 75,451 nodes, are employed. Figs. 13 and 14 illustrate the distribution of temperature at time points 240 s and 960 s, respectively. In these figures, the units of temperature are degrees centigrade (°C).

To show the results more accurately, Table 1 listed the temperature on some sample points (which is distributed along a line across one axis of the crank).

From the figures and the data listed in the table, it can be concluded that the results obtained by the BFM coincide nicely with that obtained by the ABAQUS. In the FEM implementation, in total 76 s including 10 s for mesh generation and 66 s for computation are consumed. The algorithm of the BFM implementation, however, can be optimized by many methods such as the fast

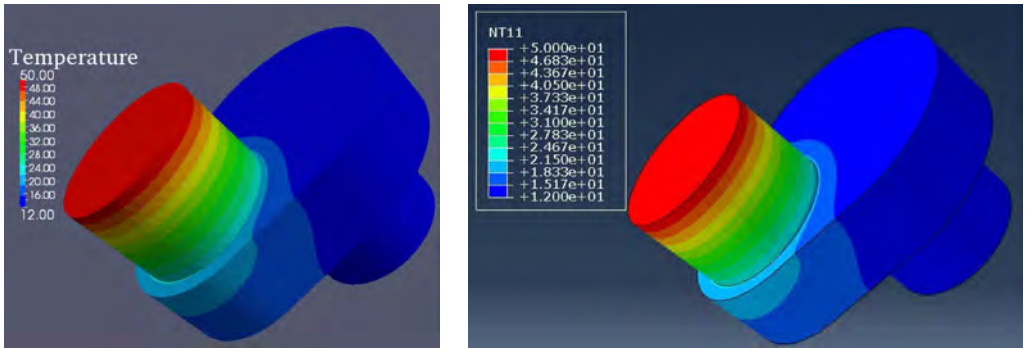

(a) (b)

Fig. 13. Temperature distribution at 240 s. (a) results obtained by BFM; (b) results obtained by ABAQUS.

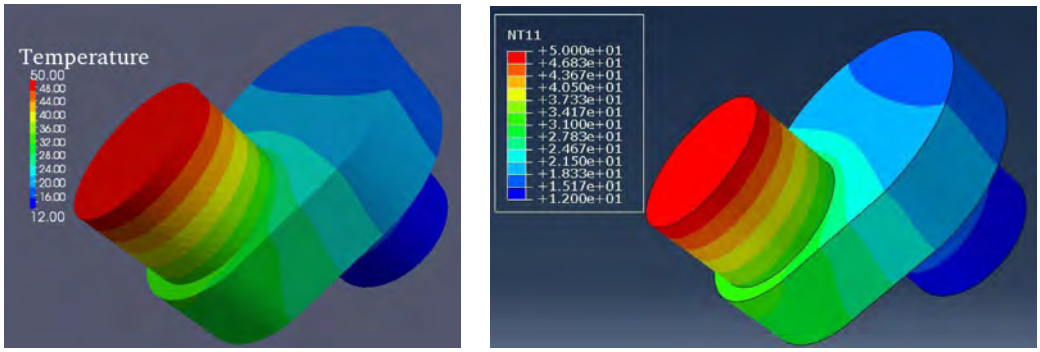

Fig. 14. Temperature distribution at 960 s. (a) results obtained by BFM; (b) results obtained by ABAQUS.

Table 1
Temperatures (°C) on the sample points at 240 s and 960 s.

	240 s		960 s	
	FEM	BFM	FEM	BFM
(0,560,219.2)	50.00	50.00	50.00	50.00
(0,490,219.2)	38.35	38.96	42.95	43.71
(0,420,219.2)	29.72	30.40	37.68	38.17
(0,350,219.2)	23.29	23.45	33.32	33.73
(0,280,219.2)	18.02	18.31	30.16	30.35

multi-pole method and the hierarchical matrix method which is our ongoing work. This example demonstrated that the proposed method is suitable for transient heat conduction problem on engineering structures.

6. Conclusion and future work

This paper proposed a time step amplification method to solve the numerically unstable problem that appears in the application of quasi-initial condition method. In this time step amplification method, the time step which is applied in the computation is larger than the considered time step. The boundary condition at the virtual time point was obtained through a linear interpolation scheme. Thus the computed result can satisfy both the governing equation and the boundary condition. Three examples were presented to illustrate the accuracy, the efficiency and the applicability of the proposed method. By equipping with the proposed method, the stability of the quasi-initial condition method has been largely improved without much loss of accuracy. The ability of the proposed method for engineering transient heat conduction problem has been illustrated in the last example through a comparison with the FEM implementation.

The time step amplification method is efficient. The evaluation of the amplification scale, however, should be further studied. Improper scale will lead to an unacceptable result. Furthermore, reasons which cause the instability, however, will be studied in our ongoing work.

Conflict of interest

None declared.

Acknowledgments

This work was supported by National Science Foundation of China under Grant numbers 11172098 and 51374101 and National 973 Project of China under Grant number 2010CB328005.

References

[1] Y. Jaluria, K.E. Torrance, Computational Heat Transfer, Hemisphere Publication Corporation, Washington, 1986.
[2] D.A. Anderson, J.C. Tannehill, R.H. Pletcher, Computational Fluid Mechanics and Heat Transfer, Hemisphere Publication Corporation, Washington, 1997.
[3] H.K. Versteeg, W. Malalasekera, An Introduction to Computational Fluid Dynamics. The Finite Volume Method, Longman Scientific & Technical, Essex, 1995.
[4] W.Q. Tao, Recent Advances in Computational Heat Transfer, Science Press, Beijing, 2000. in Chinese.
[5] J.N. Reddy, D.K. Gartling, The Finite Element Method in Heat Transfer and Fluid Dynamics, CRC Press LLC, 2010.
[6] R.W. Lewis, K. Morgan, H.R. Thomas, et al., The Finite Element Method in Heat Transfer Analysis, Wiley, 1996.
[7] A. Sutradhar, G.H. Paulino, L.J. Gray, Transient heat conduction in homogeneous and non-homogeneous materials by the Laplace transform Galerkin boundary element method, Eng. Anal. Bound. Elem. 26 (2002) 119–132.
[8] L.R. Hill, T.N. Farris, Fast Fourier transform of spectral boundary elements for transient heat conduction, Int. J. Numer. Methods Heat Fluid Flow 5 (1995) 813–827.
[9] S.P. Guo, J.M. Zhang, G.Y. Li, et al., Three dimensional transient heat conduction analysis by Laplace transformation and multiple reciprocity boundary face method, Eng. Anal. Bound. Elem. 37 (2013) 15–22.
[10] R.H. Thaler, W.K. Mueller, A new computational method for transient heat conduction in arbitrarily shaped regions, in: Fourth International Heat Transfer Conference, Elsevier Publishing Co., Amsterdam, 1970.
[11] C.A. Brebbia, J.C.F. Telles, L.C. Wrobel, Boundary Element Techniques: Theory and Applications in Engineering, Springer-Verlag, Berlin and New York, 1984.
[12] M.T. Ibanez, H. Power, An efficient direct BEM numerical scheme for heat transfer problems using Fourier series, Int. J. Numer. Methods Heat Fluid Flow 10 (2000) 687–720.
[13] A. Gupta, J.M. Sullivan, H.E. Delgado, An efficient BEM solution for three dimensional transient heat conduction, Int. J. Numer. Methods Heat Fluid Flow 5 (1995) 327–340.
[14] F. Ma, J. Chatterjee, D.P. Henry, P.K. Banerjee, Transient heat conduction analysis of 3D solids with fiber inclusions using the boundary element method, Int. J. Numer. Methods Eng. 73 (2008) 1113–1136.
[15] F.L. Zhou, G.Z. Xie, J.M. Zhang, et al., Transient heat conduction analysis of solid with small open-ended tubular cavities by boundary face method, Eng. Anal. Bound. Elem. 37 (2013) 542–550.
[16] C.H. Wang, M.M. Grigoriev, G.F. Dargush, A fast multi-level convolution boundary element method for transient diffusion problems, Int. J. Numer. Methods Eng. 62 (2005) 1895–1926.
[17] G.F. Dargush, P.K. Banerjee, Application of the boundary element method to transient heat conduction, Int. J. Numer. Methods Eng. 31 (1991) 1231–1247.
[18] J.M. Zhang, X.Y. Qin, X. Han, G.Y. Li, A boundary face method for potential problems in three dimensions, Int. J. Numer. Methods Eng. 80 (2008) 320–337.
[19] X.Y. Qin, J.M. Zhang, G.Y. Li, X.M. Sheng, Q. Song, A finite element implementation of the boundary face method for potential problems in three dimensions, Eng. Anal. Bound. Elem. 34 (2010) 934–943.
[20] X.Y. Qin, J.M. Zhang, L.P. Liu, Steady-state heat conduction analysis of solids with small open-ended tubular holes by BFM, Int. J. Heat Mass Transfer 55 (2012) 6846–6853.
[21] F.L. Zhou, J.M. Zhang, X.M. Sheng, G.Y. Li, Shape variable radial basis function and its application in dual reciprocity boundary face method, Eng. Anal. Bound. Elem. 35 (2011) 244–252.
[22] J.L. Gu, J.M. Zhang, G.Y. Li, Isogeometric analysis in BIE for 3-D potential problem, Eng. Anal. Bound. Elem. 36 (2012) 858–865.
[23] K. Onishi, Convergence in the boundary element method for heat equation, TRU Math. 17 (1981) 213–225.

[24] S. Sharp, Stability analysis for boundary element methods for the diffusion equation, Appl. Math. Modell. 10 (1986) 41–48.
[25] A.P. Peirce, A. Askar, H. Rabitz, Convergence properties of a class of boundary element approximations to linear diffusion problems with localized nonlinear reactions, Numer. Methods Partial Diff. Equ. 6 (1990) 75–108.
[26] G.F. Dargush, M.M. Grigoriev, Higher-order boundary element methods for transient diffusion problems. Part II: Singular flux formulation, Int. J. Numer. Methods Eng. 55 (2002) 41–54.